

NUMERICAL SIMULATION OF THE FLOW AROUND A KAYAK HULL

Alexandra Madalina Bujor

“Dunarea de Jos” University of Galati,
Faculty of Naval Architecture, Galati, Domneasca
Street, No. 47, 800008, Romania,
E-mail:mb389@student.ugal.ro

Andreea Mandru

“Dunarea de Jos” University of Galati,
Faculty of Naval Architecture, Galati, Domneasca
Street, No. 47, 800008, Romania,
E-mail:andreea.mandru@ugal.ro

Florin Pacuraru

“Dunarea de Jos” University of Galati,
Faculty of Naval Architecture, Galati, Domneasca
Street, No. 47, 800008, Romania,
E-mail:florin.pacuraru@ugal.ro

ABSTRACT

The purpose of this study was to determine the total resistance and investigate the flow around a full-scale kayak. Utilizing Computational Fluid Dynamics (CFD), it was determined how the presence of a rudder affects the kayak's hydrodynamic performance. To analyse the flow, computational fluid dynamics based on the RANS-VOF solver were employed. The fluid volume approach and the $k-\omega$ turbulence model were used in two-phase steady flow simulations around the kayak hulls.

Keywords: sea kayak, numerical simulation, RANSE, CFD.

1. INTRODUCTION

A kayak is a lightweight craft that works well on moving or still water, as well as near the coast. It originated in the icy regions of Greenland. There are two distinct types of kayaks, each of which can be further subdivided: sea kayaking or touring and racing or sport kayaks.

Touring requires a kayak that maintains a straight course without requiring energy-sapping correction strokes. In order to cover the distance while expending the least amount of energy, the kayak must move quickly. It needs inertia to continue moving at the desired speed when it is hit by waves or wind. It must be capable of carrying supplies for long cruises.

Considering that no empirical methods are available to predict the resistance of the

kayaks, the computational fluid dynamics (CFD) method is one of the most efficient and cost-effective approaches for examining hydrodynamic performance among the various techniques that aid in the improvement of the kayak hull design. Although it is possible to calculate the total resistance, previous research has not been able to properly explain the complex viscous flow around the kayak hull. The findings of earlier breakthroughs are still quite rough, despite the quick adoption of CFD in large boats and ships, and a few recent advancements in the research of viscous flow around kayaks are helping to enhance the design [1].

Over the past two decades, computational fluid dynamics (CFD) has been used extensively. Due to significant improvements in physical and numerical modelling techniques, it is now possible to study and inves-

tigate more complex ship hydrodynamic problems at both model and full-scale levels. This development has also been accompanied by a significant improvement in computational methods. Recent advances in computing power have given rise to High Performance Computing (HPC), enabling the use of smaller grids, fewer physical modelling assumptions, and faster simulation. Also, a better understanding of computational flows and uncertainties based on rigorous verification and validation methods has made it easier to trust the results of numerical simulations and made it easier to understand and solve problems with numerical simulations [2].

The configurations of tow kayaks, as shown in figure 1, were investigated, and the main geometric characteristics are listed in Table 1. The first configuration (V1) is a bare hull without appendages. The second one (V2) is the V1 hull with a rudder.

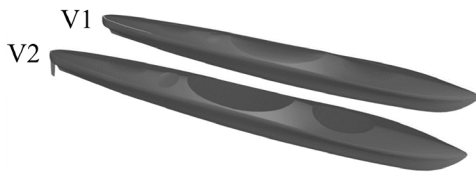


Fig.1. Hull geometry

Table 1. Main particulars of the kayak hull

Main Particulars	V1	V2
Length overall – L _{OA} [m]	5.000	
Beam - B [m]	0.560	
Draft - T [m]	0.168	
Depth moulded- D [m]	0.380	
Wetted surface [m ²]	2.025	2.042

2. NUMERICAL APPROACH

2.1. Governing equations

In this study, the ISIS-CFD viscous flow CFD solver from the FINETM/Marine package, sold under the NUMECA name, was employed for all numerical simulations. In order to solve the Reynolds-Averaged Navier-Stokes equations in a global approach, the solver uses the finite volume method to build the spatial discretization for the governing equation [3]. The flows are built using a face-to-face method, allowing the solver to employ any control volume with any form [4].

The averaged continuity and momentum equations for incompressible flows, including external forces (1 and 2), can be expressed in tensor form as:

$$\frac{\partial(\rho \bar{u}_i)}{\partial x_i} = 0 \quad (1)$$

$$\frac{\partial(\rho \bar{u}_i)}{\partial t} + \frac{\partial}{\partial x_j} (\rho \bar{u}_i \bar{u}_j + \overline{\rho u_i' u_j'}) = - \frac{\partial \bar{p}}{\partial x_i} + \frac{\partial \bar{\tau}_{ij}}{\partial x_j} \quad (2)$$

where ρ is density, u_i is the relative averaged velocity vector of flow between the fluid and the control volume, $u_i' u_j'$ is the Reynolds stresses, \bar{p} is the mean pressure and τ_{ij} is the mean viscous stress tensor component for Newtonian fluid under the incompressible flow assumption, and it can be written as in equation 3:

$$\bar{\tau}_{ij} = \mu \left(\frac{\partial \bar{u}_i}{\partial x_j} + \frac{\partial \bar{u}_j}{\partial x_i} \right) \quad (3)$$

in which μ is the dynamic viscosity.

2.2. Computational grid

To discretize the computational domain, the HEXPRESSTM module of the FINETM/Marine package was used to generate an unstructured hexahedral grid. The val-

idation case parameters are used to initiate the process of grid generation; for instance, the ship's speed corresponds to $Fr = 0.146$. Given that, the other test cases are subject to a higher velocity and that the refinement parameters for the area surrounding the free surface and the hull will be sufficient by default, this is considered acceptable from the perspective of numerical grid generation. The grid is created with adequate vertical refinement to structure the wave system for a zero-degree starting trim.

A high-quality grid is essential for obtaining accurate numerical results. To cover the entire computational domain, a preliminary unstructured Cartesian grid was created. The H-H type grid topology is used. Figure 2 depicts the distribution of cells across the bow, stern, and rudder. Also, it can be seen that the finer mesh is applied in the area where the kayak wave system develops. For each kayak configuration, two grids that cover the entire computational domain were generated, with the number of cells ranging from 1.2 to 2.1 million.

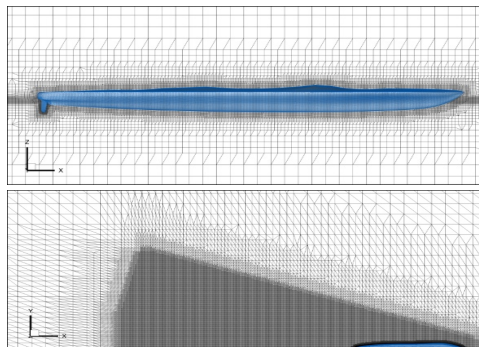


Fig.2. Computational mesh generated around the kayak hull

3. RESULTS AND DISCUSSIONS

In the following, the results of the numerical simulations performed for the three kayak configurations are presented.

3.1. Pilot test case

A bare hull without any appendages was used in the first computations to analyze the flow around it and calculate the drag. Five different speeds with Froude numbers ranging from 0.146 to 0.293 were calculated.

As a result, the values of velocity (v) and the related Froude number (Fn), as well as the values of wave resistance (R_w), viscous resistance (R_v), and total resistance (R_t), are listed in Table 2.

Table 2. Results of numerical simulations for V1 configuration

v [Kn]	Fn	R_t [N]	R_w [N]	R_v [N]
2	0.146	3.849	0.328	3.520
2.5	0.183	6.183	0.867	5.316
3	0.220	9.223	1.777	7.446
3.5	0.256	12.987	3.035	9.952
4	0.293	17.258	4.359	12.898

The total resistance curve is plotted in Figure 3, and Figure 4 illustrates the wave elevation at various Froude numbers.

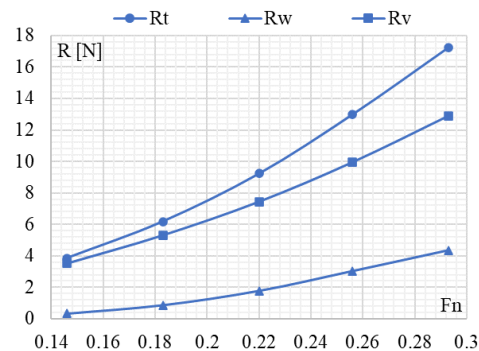


Fig.3. Total resistance, wave resistance and viscous resistance curves for V1

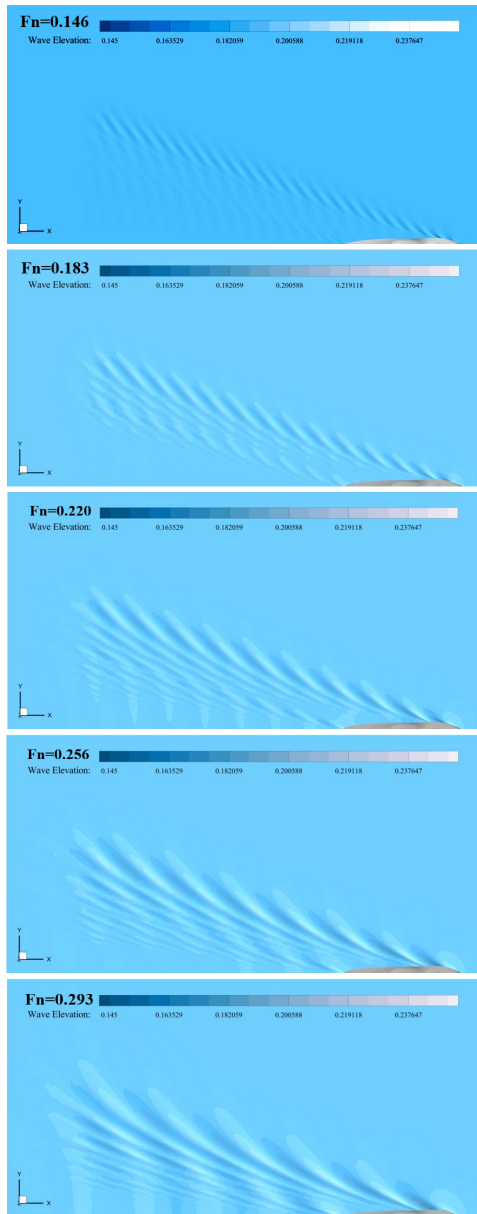


Fig.4. Wave elevation of the V1 kayak configuration for different Froude number

3.2. The effect of rudder on total resistance

For the second set of computations, the V1 hull with a rudder was used to analyze the flow around it and to evaluate the effect

of the rudder on the total resistance. Five different speeds with Froude numbers ranging from 0.146 to 0.293 were calculated.

The rudder is located at the kayak's stern, is designed to pivot from side to side, and is controlled by pedals connected by cables made of stainless steel or other durable materials. The rudder makes the kayak much easier to steer, requires less effort to maintain direction, and facilitates manoeuvrability. The system allows the rudder to be pulled up, which makes it retractable [5].

The numerical simulation results for configuration V2 were compared with those obtained for configuration V1 and are listed as follows: Table 3 presents the comparison for total resistance and Table 4, the comparison for viscous resistance. Figure 5, Figure 6 and Figure 7 represent the comparison between the total resistance curves, wave resistance curves, respectively viscous resistance curves. Also, Figure 8 illustrates the wave elevation at various Froude numbers. It can be observed that the presence of the rudder leads to an increase in drag of up to 10%.

Table 3. Total resistance - comparison between V1 and V2

v [Kn]	Fn	V1_R _t [N]	V2_R _t [N]	R _t [%]
2	0.146	3.849	4.258	10.60
2.5	0.183	6.183	6.825	10.37
3	0.220	9.223	10.150	10.04
3.5	0.256	12.987	14.283	9.97
4	0.293	17.258	18.995	10.06

Table 4. Viscous resistance - comparison between V1 and V2

v [Kn]	Fn	V1_R _v [N]	V2_R _v [N]	R _v [%]
2	0.146	3.520	3.536	0.45
2.5	0.183	5.316	5.339	0.43
3	0.220	7.446	7.472	0.35
3.5	0.256	9.952	9.985	0.33

4	0.293	12.898	12.932	0.26
---	-------	--------	--------	------

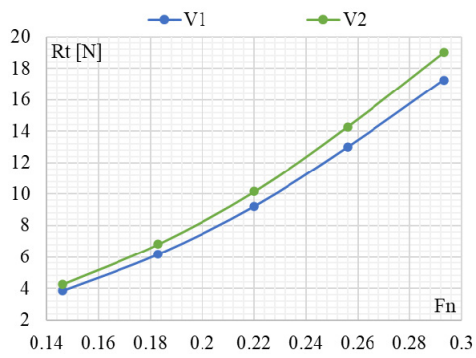


Fig.5. Total resistance - comparison between V1 and V2

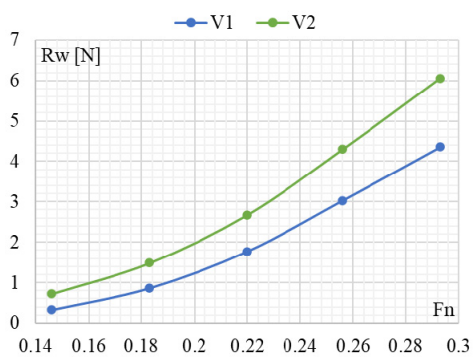


Fig.6. Wave resistance - comparison between V1 and V2

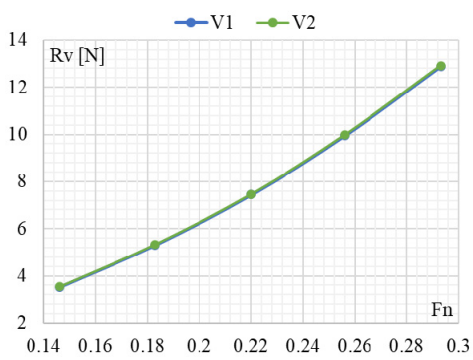


Fig.7. Viscous resistance - comparison between V1 and V2

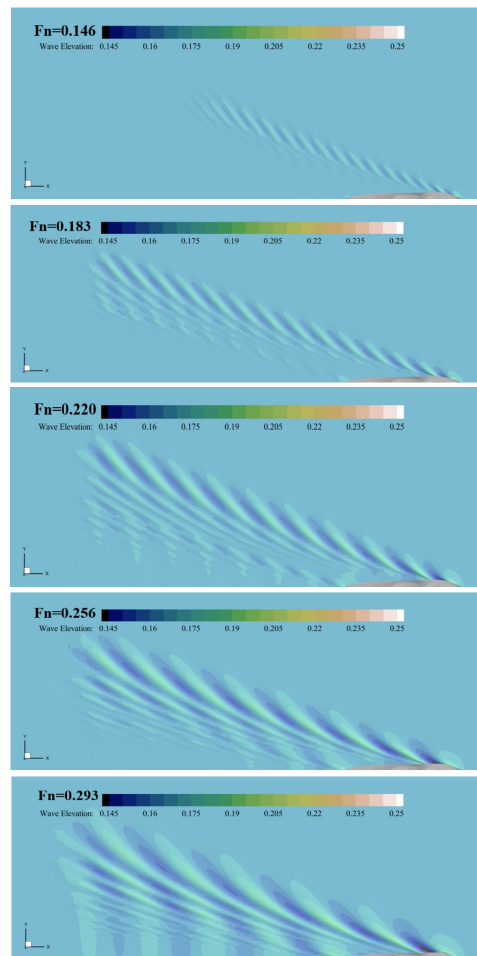


Fig.8. Wave elevation of the V2 kayak configuration for different Froude number

4. CONCLUDING REMARKS

In this paper, numerical investigations on the sea kayak's hydrodynamic performance were conducted, counting 10 computational cases.

The free surface flow around the kayak and the influence of the presence of the rudder have been successfully investigated by means of numerical simulations based on the RANS-VOF method. The drag as well as the topology of the free surface have been analysed for a range of velocities corresponding

to the Froude number interval between 0.146 and 0.293.

The influence of the presence of the rudder on the hydrodynamic parameters was studied by comparison with the results obtained for flow around the bare kayak hull. Thus, it can be observed that the presence of a rudder leads to an increase in drag by up to 10%.

REFERENCES

- [1]. **Mantha, V., R., Silva, A., J., Marinho, D., A., Rouboa, A., I.**, "Numerical Simulation of Two-Phase Flow Around Flatwater Competition Kayak Design- Evolution Models", *Journal of Applied Biomechanics*, 29, pp 270-278, 2013.
- [2]. **Queutey, P., Visonneau, M.**, "An interface capturing method for free-surface hydrodynamic flows", *Computers & Fluids*, 36(9) pp 1481–1510, 2017.
- [3]. **Guilmineau, E., Deng, G., B., Leroyer, A., Queutey, P., Visonneau, M., Wackers, J.**, "Influence of the turbulence closures for the wake prediction of a marine propeller", *Proc. of the 4th International Symposium on Marine Propulsors*, 2015.
- [4]. **Duvigneau, R., Visonneau, M., Deng, G., B.**, "On the role played by turbulence closures in hull shape optimization at model and full-scale", *J. Marine Science and Technology*, 8 (1), 1–25, 2003.
- [5]. <https://www.kayarchy.com/html/01equipme nt/016almostessential.htm>

Paper received on November 20th, 2022